Synthesis of Hexagonal Nanophases in the La_2O_3 – MO_3 (M = Mo, W) Systems

Baldin E. D.[1], Lyskov N.V.[2,3], Vorobieva G.A.[1], Kolbanev I.V.[1], Karyagina O.K.[4], Stolbov D.N.[5], Voronkova V.I.[6], Shlyakhtina A.V.[1]

1 - N.N. Semenov Federal Research Center for Chemical Physics, Russian Academy of Sciences, Moscow, Russia
2 - Federal Research Center of Problems of Chemical Physics and Medical Chemistry RAS, Moscow region, Chernogolovka, Russia
3 - National Research University "Higher School of Economics", Moscow, Russia
4 - Emanuel Institute of Biochemical Physics RAS, Moscow, Russian Academy of Sciences, Russia
5 - Department of Chemistry, Lomonosov Moscow State University, Moscow, Russia
6 - Department of Physics, Lomonosov Moscow State University, Moscow, Russia

ABSTRACT

We report a study of nanophases in the La_2O_3-MO_3 (M = Mo, W) systems, which are known to contain a variety of good oxygen-ion and proton conductors. Mechanically activated La_2O_3+MO_3 (M = Mo, W) mixtures have been characterized by DSC and XRD with Rietveld refinement, the microstructure of the materials has been examined by SEM, and their conductivity in dry and wet air has been determined using impedance spectroscopy. In both systems, the formation of hexagonal $La_{15}M_{8.5}O_{48}$ (phase II, 5H polytype) (M = Mo, W) nanophases is observed for composition 1:1, with exothermic peaks in the DSC curve in the range ~480–520 °C for $La_{15}Mo_{8.5}O_{48}$ and ~ 685–760 °C for $La_{15}W_{8.5}O_{48}$. The crystallite size of the nanocrystalline tungstates is ~40 nm and that of the nanocrystalline molybdates is ~50 nm. At higher temperatures (~630–690 and ~1000 °C), we observe irreversible reconstructive phase transitions of hexagonal $La_{15}Mo_{8.5}O_{48}$ to tetragonal γ- La_2MoO_6 and of hexagonal $La_{15}W_{8.5}O_{48}$ to orthorhombic β-La_2WO_6. We compare temperature dependences of conductivity for nanoparticulate and microcrystalline hexagonal phases and high-temperature phases differing in density. Above 600 °C, oxygen ion conduction prevails in the coarse-grained $La_{18}W_{10}O_{57}$ (phase I, 6H polytype) ceramic. Low-density $La_{15}W_{8.5}O_{48}$ and $La_{15}Mo_{8.5}O_{48}$ (phase II, 5H polytype) nanoceramics exhibit predominantly electron conduction with an activation energy of 1.36 and 1.35 eV, respectively, in dry air.

Particle size and morphology of starting oxide powders and mechanically activated powders

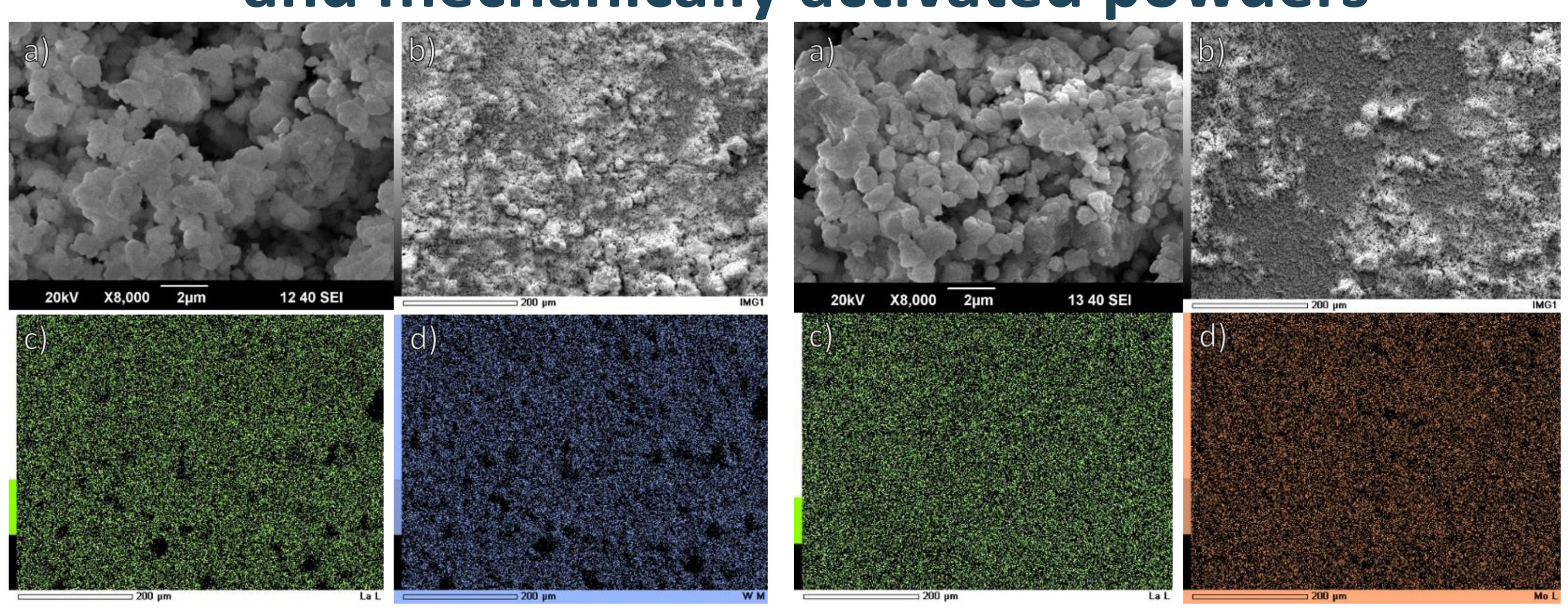

Fig. 1 SEM image (a) (magnification 2 μm) and (b) (magnification 200 μm), (c ,d) La and M X-ray maps of the mechanically activated (m/a) La_2O_3+MO_3 oxide mixture. W (left), Mo (right)

Thermal analysis

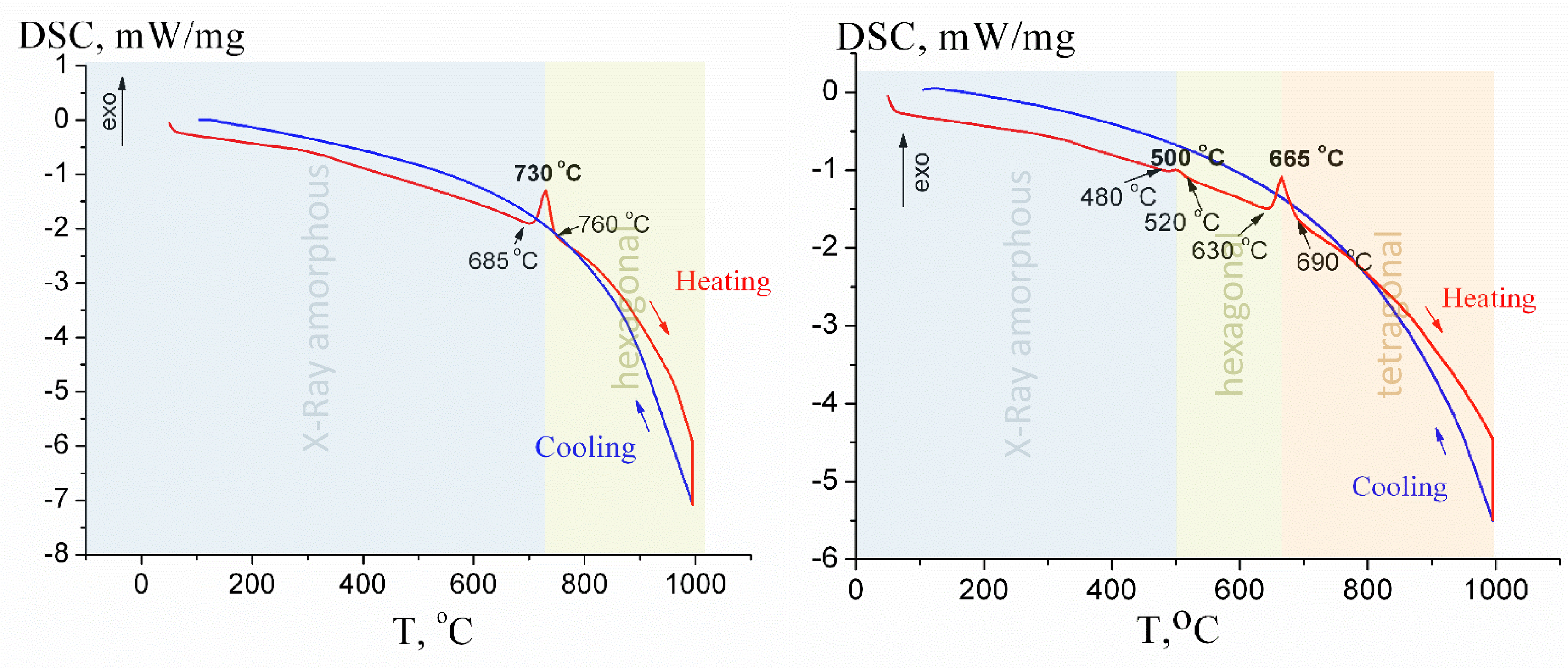

Fig. 2 Data obtained in a DSC cell during heating to 1000 °C, illustrating the exothermic process in a mechanically activated La_2O_3+MO_3 mixture. M = W (left), Mo (right)

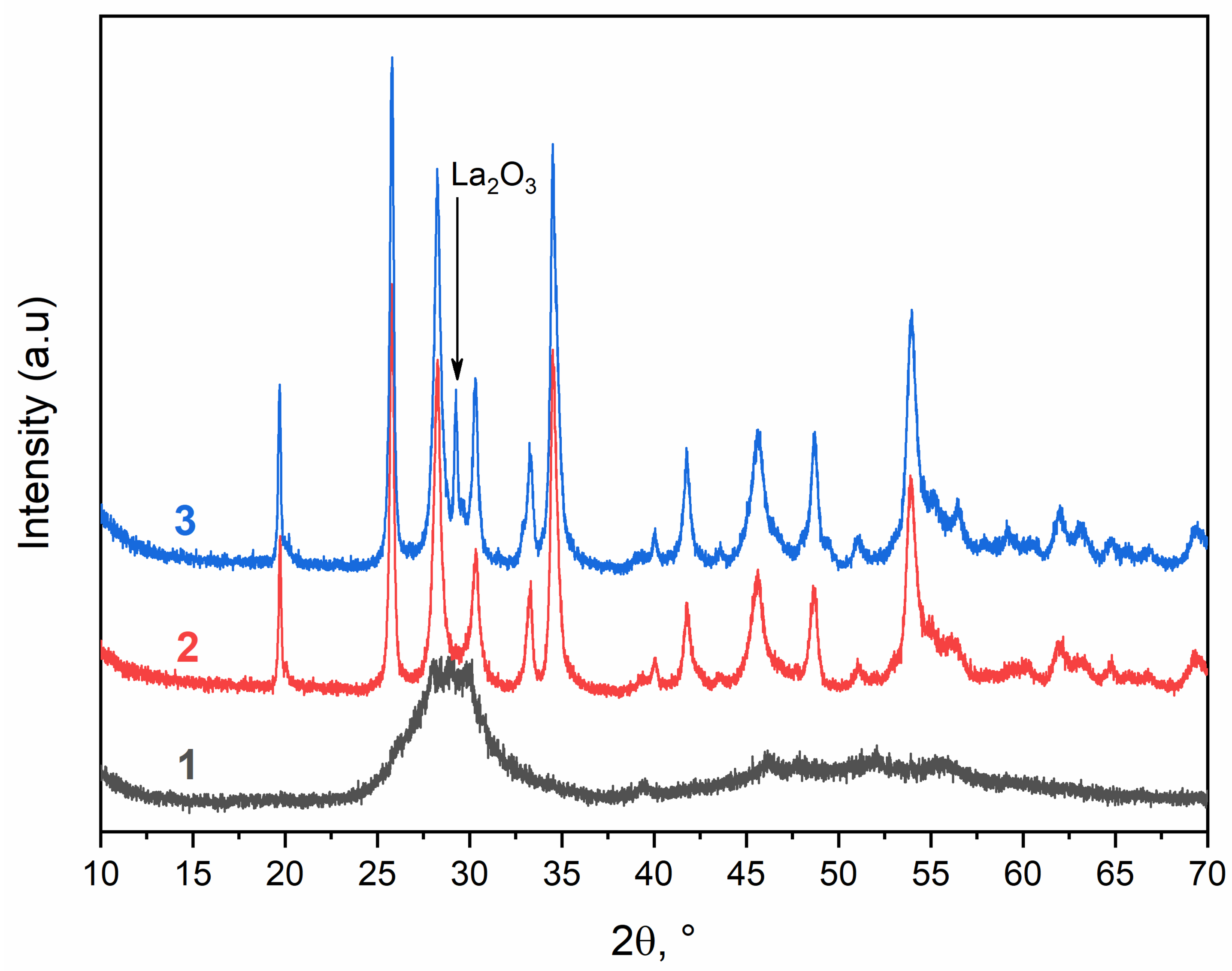

Fig. 3 XRD patterns of mechanically activated (m/a) La2O3+WO_3 mixture (1) after heating in DSC cell up to 685 °C, (2) after heating in DSC cell up to 760 °C, (3) after thermal annealing at 600 °C for 96 h. La_2O_3 (ICDD PDF 1523968) - 41.1(6) wt.%.

X-Ray Powder Diffraction

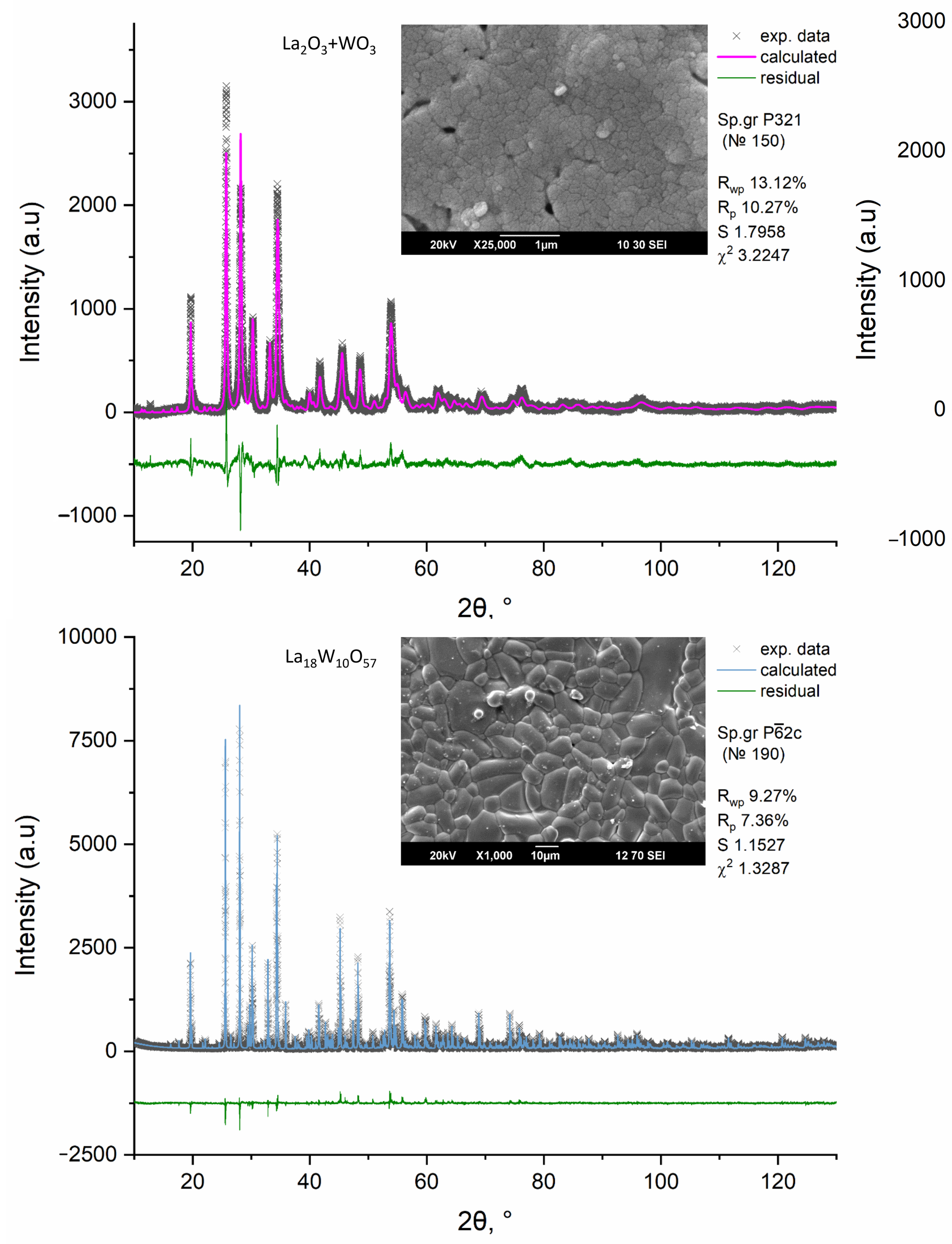

Fig. 4 Rietveld refinement of the XRD pattern of the m/a La_2O_3+WO_3 mixture after annealing at 800 °C for 4h, La_2O_3+MoO_3 — 600 °C for 4h. $La_{18}W_{10}O_{57}$ (polytype 6H, phase I) sample synthesized at 1400 °C for 4 h. Crosses represent the observed pattern, the solid line through the symbols shows the calculated fit. The difference between the observed and calculated data is shown at the bottom.

Ionic conductivity

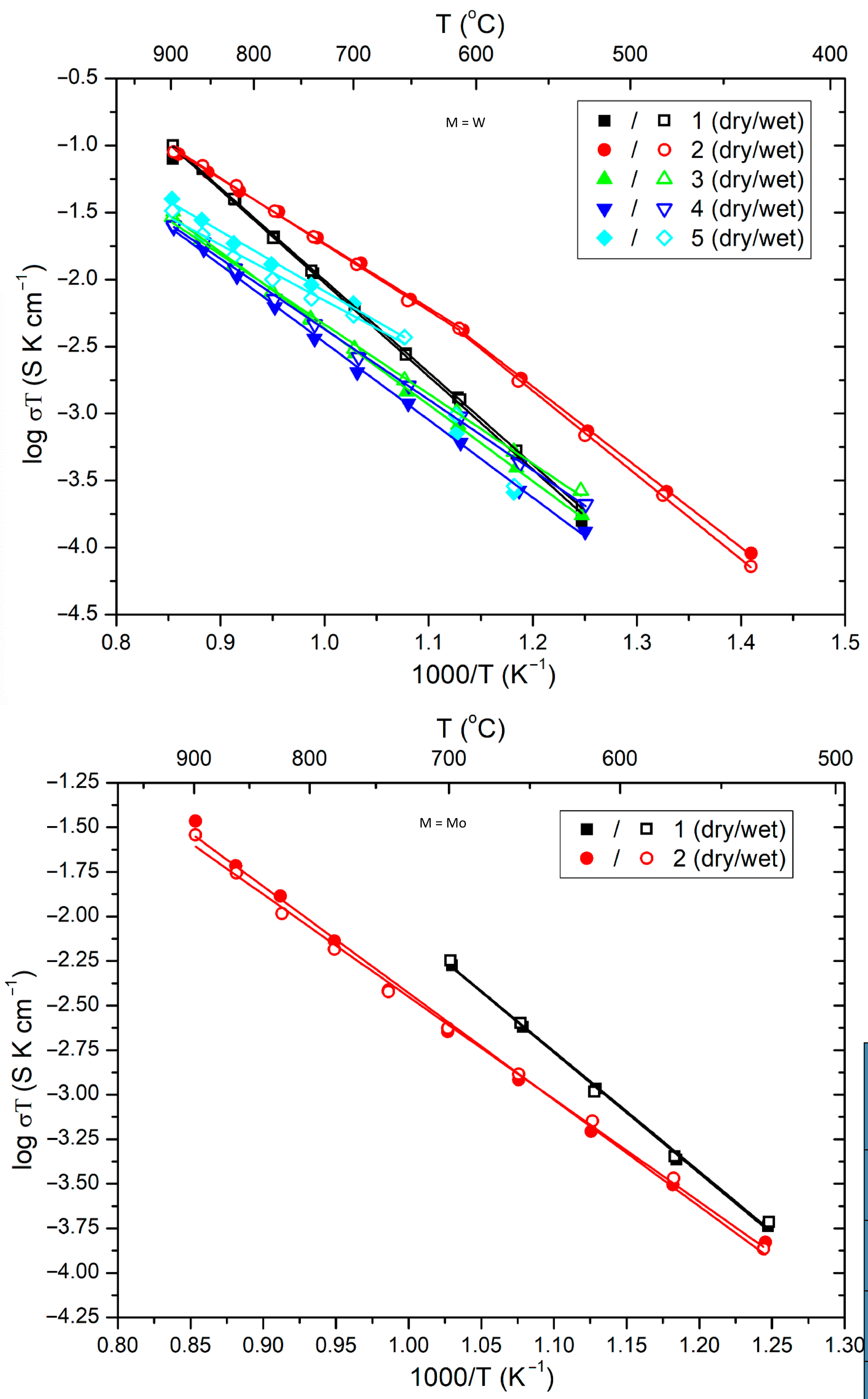

Fig. 5 Arrhenius plots of total conductivity for LaMO materials in dry (filled data points) and wet (open data points) air: **Top** (1) low-density hexagonal $La_{15}W_{8.5}O_{48}$ nanoceramic (relative density of 60.0%), (2) dense coarse-grained $La_{18}W_{10}O_{57}$ ceramic (relative density of 92%), (3) low-density orthorhombic β-La_2WO_6 ceramic (relative density of 69.6%), (4) coarse-grained orthorhombic β-La_2WO_6 ceramic (relative density of 81.4%) and (5) $La_2W_{1+x}O_{6+3x}$ (*x* ~ 0.22) single crystal. **Bottom** (1) low-density hexagonal $La_{15}Mo_{8.5}O_{48}$ nanoceramic (relative density of 64.8%) and (2) low-density tetragonal γ-La_2MoO_6 ceramic (relative density of 69.6%)

<table>
<tr><th colspan="2" rowspan="2">Composition, $T_{synthesis}$</th><th colspan="2">E_a (±0.01), eV</th></tr>
<tr><th>400–600 °C</th><th>600–900 °C</th></tr>
<tr><td rowspan="2">$La_{15}W_{8.5}O_{48}$ – 800 °C</td><td>Dry air</td><td colspan="2">1.36</td></tr>
<tr><td>Wet air</td><td colspan="2">1.35</td></tr>
<tr><td rowspan="2">$La_{18}W_{10}O_{57}$ – 1400 °C</td><td>Dry air</td><td>1.19</td><td>0.96</td></tr>
<tr><td>Wet air</td><td>1.25</td><td>0.98</td></tr>
<tr><td rowspan="2">β-La_2WO_6 – 1000 °C</td><td>Dry air</td><td colspan="2">1.13</td></tr>
<tr><td>Wet air</td><td colspan="2">1.03</td></tr>
<tr><td rowspan="2">β-La_2WO_6 – 1400 °C</td><td>Dry air</td><td colspan="2">1.16</td></tr>
<tr><td>Wet air</td><td colspan="2">1.05</td></tr>
<tr><td rowspan="2">$La_2W_{1+x}O_{6+3x}$ (x ~ 0.22) single crystal</td><td>Dry air</td><td></td><td>0.89</td></tr>
<tr><td>Wet air</td><td></td><td>0.83</td></tr>
<tr><th colspan="2"></th><th>500–700 °C</th><th>500–900 °C</th></tr>
<tr><td rowspan="2">$La_{15}Mo_{8.5}O_{48}$ – 600 °C</td><td>Dry air</td><td>1.35</td><td></td></tr>
<tr><td>Wet air</td><td>1.34</td><td></td></tr>
<tr><td rowspan="2">γ-La_2MoO_6 – 900 °C</td><td>Dry air</td><td></td><td>1.14</td></tr>
<tr><td>Wet air</td><td></td><td>1.09</td></tr>
</table>

Funding

The support of this work from Russian Foundation for Basic Research (Project 20-03-00399) is gratefully acknowledged. The work was supported partially by the subsidy from the Ministry of Education and Science allocated by the FRC CP RAS for the implementation of the state assignment (No.122040500071-0, No. 122040500068-0) and in accordance with the state task for FRC PCP and MC RAS, state registration No. AAAA-A19-119061890019-5. L.N.V. acknowledges the project of the HSE Scientific and Educational Group (No. 23-00-001).